Enhanced Diapycnal Mixing by Salt Fingers in the Thermocline of the Tropical Atlantic

R. W. Schmitt,* J. R. Ledwell, E. T. Montgomery, K. L. Polzin, J. M. Toole

Diapycnal mixing plays a significant role in the ocean's circulation and uptake of heat and carbon dioxide, but has not been quantified in salt finger–driven thermohaline staircases. We recently performed a tracer release experiment in the western tropical Atlantic staircase at ~400 m depth. The observed dispersion implies an effective diapycnal diffusivity for tracer and salt of 0.8 to 0.9 × 10^{-4} m^2/s. Temperature microstructure data interpreted in terms of a vertical production-dissipation balance yields a smaller effective diffusivity for heat of 0.45 (± 0.2) × 10^{-4} m^2/s, consistent with salt fingers and well above the mixing ascribable to mechanical turbulence.

Since the discovery of salt fingers by Stern (*1*) in 1960, there has been much speculation about their role in oceanic mixing (*2*, *3*). Fieldwork has suggested the importance of salt fingers to the dynamics of fine scale intrusions (*4*) and in regional water mass transformations (*5*–*7*), but their contribution to the rates of diapycnal mixing has not been quantified. The difficulty has been due in part to uncertainties in the methods of measuring and interpreting oceanic microstructure for double-diffusive mixing. Because tracer release experiments (TREs) are complementary to the analysis of microstructure data, they offer an independent means of quantifying diapycnal mixing in the ocean. TREs have been successfully carried out in an eastern subtropical gyre area [the North Atlantic Tracer Release Experiment, NATRE (*8*, *9*)] and an abyssal region above rough bathymetry (*10*, *11*). To address the salt finger question, we recently performed a TRE in the western tropical North Atlantic where warm, high-salinity Subtropical Underwater overlies cooler, fresher Antarctic Intermediate Water (*5*, *12*). Here the stratification through the main thermocline is often characterized by 10 or more layers (each 10 to 30 m thick), having near-uniform temperature and salinity, that are separated by 0.5- to 5-m-thick high-gradient interfaces (Fig. 1A). Such "staircase" layering in both the laboratory and ocean is a well-known manifestation of the salt finger form of double-diffusive convection (*13*), in which the greater diffusivity of heat over that of dissolved salts allows release of the potential energy of the salinity distribution in centimeter-scale convection cells.

We conducted fine structure and microstructure surveys in the western tropical Atlantic in January to February and October to December 2001 using the free-falling "high-resolution profiler" (HRP) (*14*). Temperature (T) and salinity (S) profiles from many sites revealed a step-like stratification through the main thermocline between 200 and 600 m depth (Fig. 1A). Temperature contrasts between adjacent layers sometimes approached 1°C. Staircase stratification was most commonly observed within the frontal region between the saltier North Atlantic Central Waters and fresher South Atlantic Central Waters, indicated in Fig. 2 by the salinity contour 35.1 on the density surface of the release. Our survey found a broad expanse where staircase stratification may occur that was generally consistent with the area defined by prior surveys (*5*, *12*).

The density ratio ($R_\rho = \alpha\Delta T/\beta\Delta S$, where the thermal expansion coefficient is $\alpha = \frac{-1}{\rho}\frac{\partial\rho}{\partial T}$, the haline contraction coefficient is $\beta = \frac{1}{\rho}\frac{\partial\rho}{\partial S}$, and ΔT and ΔS are the layer-to-layer temperature and salinity changes) was 1.4 to 1.7 across most interfaces, which indicates a strong propensity for salt fingering (*15*). Thermohaline staircases readily form in laboratory experiments with density ratios near one; salt fingers occupy the high-gradient interfaces and provide an up-gradient buoyancy flux that drives convective motions in the layers, maintaining weak stratification there. Thermal microstructure on the oceanic interfaces was elevated above levels normally found in the subtropical thermocline (even after accounting for the enhanced vertical temperature gradients of the interfaces). The dissipation rate of thermal variance $\left(\chi_\theta = 6\kappa_\theta\overline{\theta_z'^2}\right)$, where θ_z' represents the microscale (centimeter) fluctuations in the vertical temperature gradient, shows prominent peaks at the interfaces (Fig. 1B), although evidence for the narrow-bandwidth temperature anomalies previously seen in horizontally towed data (*16*, *17*) was lacking in these vertical profiles. A measure of the propensity for salt fingering is the theoretical salt finger growth rate that can be calculated from the separately measured meter-scale verti-

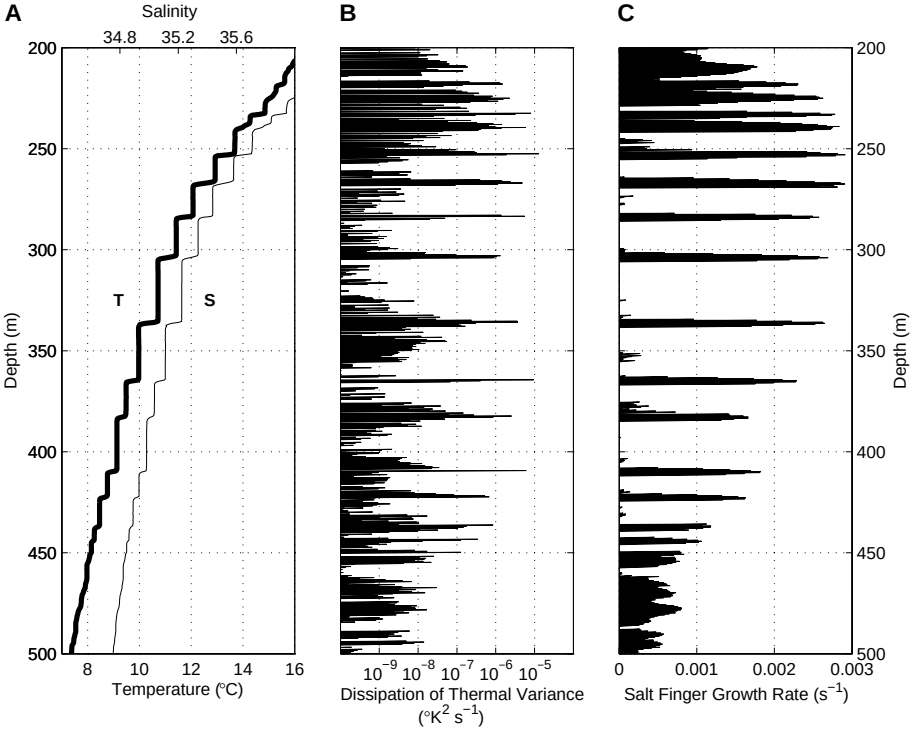

Fig. 1. Profiles of potential temperature and salinity (**A**), the dissipation rate of thermal variance (**B**), and the salt finger growth rate (**C**) for HRP dive 38 (12°24.7′N, 53°40.0′W on 7 November 2001). The SF_6 tracer was injected into the layer with potential temperature of about 10°C (centered on 350 db in this profile) in January 2001.

Woods Hole Oceanographic Institution, Woods Hole, MA 02543, USA.

*To whom correspondence should be addressed. E-mail: rschmitt@whoi.edu

cal temperature and salinity gradients (*15*) (Fig. 1C). The finger growth rate is large at the interfaces (steps) and zero in the mixed layers (risers), a pattern very similar to that of log (χ_θ). This result is consistent with the "frozen-growth" model of oceanic salt fingers (*15*, *18*).

Salt fingers transport buoyancy-scaled T and S vertically at different rates, and so, the vertical salt flux cannot be directly assessed from thermal microstructure data. Nonetheless, we infer that the normalized vertical salt flux is greater than that for heat within the staircase by inspection of the horizontal variation of temperature and salinity within the layers. As observed previously (*5*), spatial variations of temperature and salinity within a given layer are highly correlated, with the ensemble of T/S values following a distinct slope across density surfaces at an apparent lateral density ratio of 0.85. This ratio is consistent with a vertical flux divergence due to salt fingering and is not consistent with any other known oceanic mixing process (*19*). To quantify the mixing rate for salt (and other scalars) in the staircase, we released sulfur hexaflouride (SF_6) in one of the layers and measured its subsequent dispersion. SF_6 should mix like salt in the ocean because the molecular diffusivities differ by less than 10%. The advective-diffusive balances are therefore nearly the same, and so the ratio of the vertical flux to vertical gradient is expected to be the same when quantities are averaged over a volume containing many mixing events.

During the January to February 2001 cruise, 175 kg of SF_6 was released into a midstaircase layer in a patch centered near 12°45′N, 53°45′W. The layer temperature was about 10°C and salinity was about 35.1, T/S values near the median of those sampled regionally for this layer. The tracer patch was laid out with a series of eight tows of an injector sled that pumped liquid SF_6 through atomizing nozzles. Sled depth was controlled by the vessel winch with guidance from a sled-mounted conductivity-temperature-depth (CTD) instrument and additional temperature-conductivity sensors placed 10 m above and below. Tracer was pumped only when the sled was positioned within the well-mixed layer and the layer potential density anomaly was between 27.041 kg/m^3 and 27.052 kg/m^3. This initial patch fell within an area that was ~28 km in diameter. A survey completed within 2 weeks of injection indicated that nearly 92% of the tracer was in the 10°C layer, some having already mixed to neighboring interfaces and layers.

Nearly 10 months later, in October to December 2001, the tracer patch was again sampled during an extensive regional survey (Fig. 2). At each station, the SF_6 concentration in discrete water samples collected in conjunction with CTD casts was measured using electron capture gas chromatography. Concentration estimates were then adjusted to remove a background profile estimated from data obtained outside the patch. The vertical integral of adjusted SF_6 concentration was mapped over an area of 1.3×10^6 km^2. Tracer dispersal was anisotropic (strongly zonal), with SF_6 found in three main patches. About 50% of the injected tracer could be accounted for by this survey; subsequent survey work in 2003 suggested that the bulk of the "missing" tracer was in the Caribbean Sea west of the October to December 2001 survey area. The concentration profile data were subsequently integrated horizontally along isopycnals for the sampled regions east and west of the Lesser Antilles (Fig. 3). Over the 293 days between the midpoints of the injection and survey, the square root of the second moment of the vertical tracer distribution grew to 61 m. In contrast, this quantity grew to only 30 m after 12 months in the NATRE (*8*, *9*). Although the normalized concentration profiles have similar shape, the center of mass of the eastern region's distribution is about 20 m below that for the Caribbean region (and the injection isopycnal surface). This pattern appears to be partly the consequence of vertical shear in the North Equatorial Current that dominates the study region and partly the result of some sinking of the tracer.

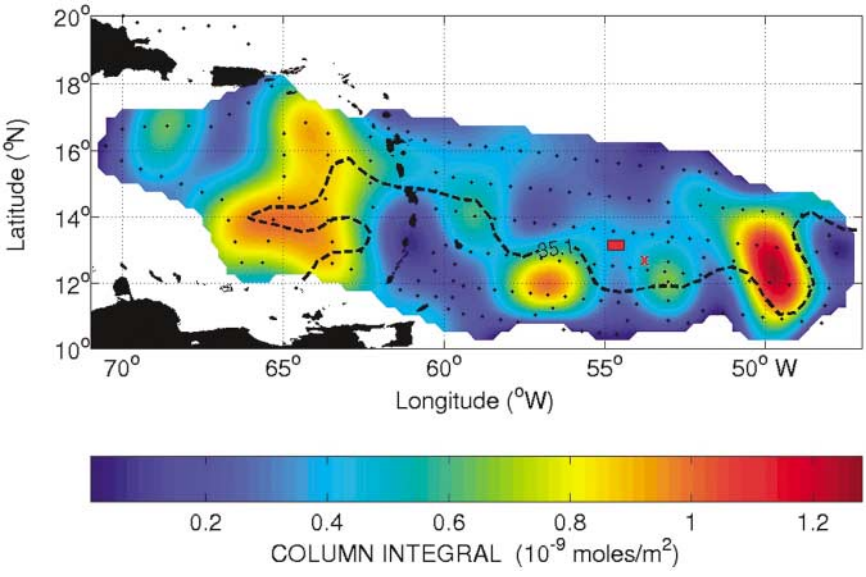

Fig. 2. Salt finger TRE map. The "X" near 54°W indicates the release area; the red rectangle northwest of the X shows the area where the tracer was found about 2 weeks after the release. The color map shows the column integral of tracer above background, in 10^{-9} mol/m^2, about 10 months after the release, with the stations shown as dots. The column integral at the stations north of the Greater Antilles was indistinguishable from background. The dashed lines indicate where the salinity was 35.1 on the density surface of the tracer release for the 10-month survey. On this surface, it is saltier to the north and fresher to the south. The tracer was not fully delimited, particularly in the northeast and the southwest.

As was described in (*9*), a model for the diapycnal dispersion was applied to the observations to diagnose the tracer's effective diapycnal diffusivity. The resulting diffusivity estimate is 0.8 to 0.9×10^{-4} m^2/s, with most of the uncertainty arising from the interpretation of the offset of the center of mass of the distribution. For reference, tracer diffusivity estimates from the eastern North Atlantic thermocline in NATRE were 0.12×10^{-4} m^2/s for the first 6 months and 0.17×10^{-4} m^2/s over 24 months. The present tracer-based estimate can be compared with the diffusivity inferred from the microstructure measurements. Several microstructure-based measures of mixing intensity are available based on the dissipation rate of thermal variance, χ_θ; the dissipation rate of turbulent kinetic energy, ε; and two different models for their interpretation: one for shear-driven turbulence and one for salt fingering. The formulae for diffusivities from the two models are as follows:

Turbulence (*20*, *21*) (with flux Richardson number, $R_f = 0.17 \pm 0.03$):

$$K_\theta = K_S = K_\rho = \frac{R_f}{1 - R_f}\frac{\varepsilon}{N^2} \approx 0.2\frac{\varepsilon}{N^2}$$

$$K_\theta = K_S = \frac{\chi_\theta}{2\overline{\theta_z}^2}$$

Salt fingers (*22*) (with $R_\rho = 1.7$ and flux ratio $\gamma = 0.75$):

$$K_S = \frac{R_\rho - 1}{1 - \gamma}\frac{\varepsilon}{N^2} \approx 2.8\frac{\varepsilon}{N^2}$$

$$K_S = \frac{R_\rho}{\gamma}\frac{\chi_\theta}{2\overline{\theta_z}^2} \approx 2.3K_\theta$$

$$K_\theta = \frac{\chi_\theta}{2\overline{\theta_z}^2}$$

In the above, K_θ, K_S, and K_ρ are the eddy diffusivities for heat, salt, and density; $N^2 = -\frac{g}{\rho}\frac{\partial \rho}{\partial z}$ is the squared buoyancy frequency, where g is gravity; and $\overline{\theta_z}$ is the mean vertical temperature gradient.

The key distinction between these two processes is found in the eddy diffusivities for heat and salt: they are equal for fully developed turbulence, but differ by a factor of ~2 for salt fingers, assuming a flux ratio of 0.75, a value consistent with laboratory, theory, and oceanic observations (*23*). From the HRP survey, overall averages of χ_θ, ε, and the vertical temperature and density gradients were formed between the potential density anomaly surfaces 26.968 and 27.128, which make up the 1-SD range of the vertical tracer spread. In this density interval $\langle\chi_\theta\rangle = 3.5 \times 10^{-8}$ K²/s, $\langle\varepsilon\rangle = 1.0 \times 10^{-9}$ W/kg, with 95% confidence intervals of 2.3 to 5.1 $\times 10^{-8}$ K²/s and 0.4 to 2.3 $\times 10^{-9}$ W/kg, respectively (*24*). These large-area average dissipations include both layers and interfaces and are somewhat larger than prior microstructure observations at one staircase site in the region (*16*, *25*), which probably reflects the greater range of phenomena likely to be observed over this wide region. The foregoing formulae yield the diffusivities shown in Table 1 when applied to these overall averages. We find best agreement between K_S inferred from the tracer dispersion and that derived by applying the salt finger model to the thermal dissipation data. The diffusivity estimated from the conventional turbulence model applied to the viscous dissipation data is a factor of five too small to explain the observed tracer dispersion.

Parts of the foregoing analysis are based on conventional vertical production-dissipation balances for temperature microstructure (*21*). Lateral stirring on isopycnal surfaces would complicate this interpretation. Within a thermohaline front, temperature and salinity anomalies can be generated by double-diffusive fluxes that cause the anomalies to migrate across density surfaces (*26*–*28*) and may even provide a mechanism for staircase formation (*29*). Such migration may account for some of the tracer dispersion and would alter the interpretation of the thermal dissipation measurements (*30*, *31*). Similarly, some fraction of the observed turbulent dissipation is likely to be contributed by internal wave processes. However, the enhanced diapycnal dispersion of SF_6 in the staircase region relative to NATRE, the strongly layered stratification with few temperature inversions, the distinct temperature-salinity relations within the layers (*5*), the enhanced thermal microstructure in the salt-finger-favorable depth intervals with small turbulent dissipation, and past evidence for bandwidth-limited microstructure in these steps (*16*, *17*) lead us to conclude that salt fingering is contributing to enhanced vertical mixing in the western tropical thermocline of the North Atlantic with an effective diapycnal diffusivity for salt and tracers twice that of heat.

The significant vertical dispersion of tracer observed in this thermohaline staircase supports the idea that salt fingers significantly enhance mixing in certain parts of the main thermocline. Our derived salt diffusivity of $0.8-0.9 \times 10^{-4}$ m²/s is an order of magnitude larger than that predicted for typical internal wave breaking within the mid-latitude thermocline. Indeed, for this low-latitude region, parameterization of mixing supported by the background internal wave field (*32*, *33*) indicates that a diffusivity of only ~0.02×10^{-4} m²/s should be expected. The tracer-derived diffusivity is also larger than that implied by microstructure measurements previously made in this staircase (*16*, *25*, *34*). However, it is in agreement with the salt finger model applied to those dissipation data (*35*), as well as to our new observations. Notably, the diapycnal tracer mixing rate observed in the western tropical Atlantic is 5 times that observed in the eastern subtropical Atlantic during NATRE, because of the presence of the thermohaline staircase. The staircase appears to transform the *T*-*S* structure of the thermocline waters entering the Caribbean, increasing the salinity and density of Antarctic Intermediate Water (*36*) and preconditioning it for sinking at higher latitudes. The efficient vertical transport within this strong tropical thermocline must be taken into account in oceanic and climate models, where the param-

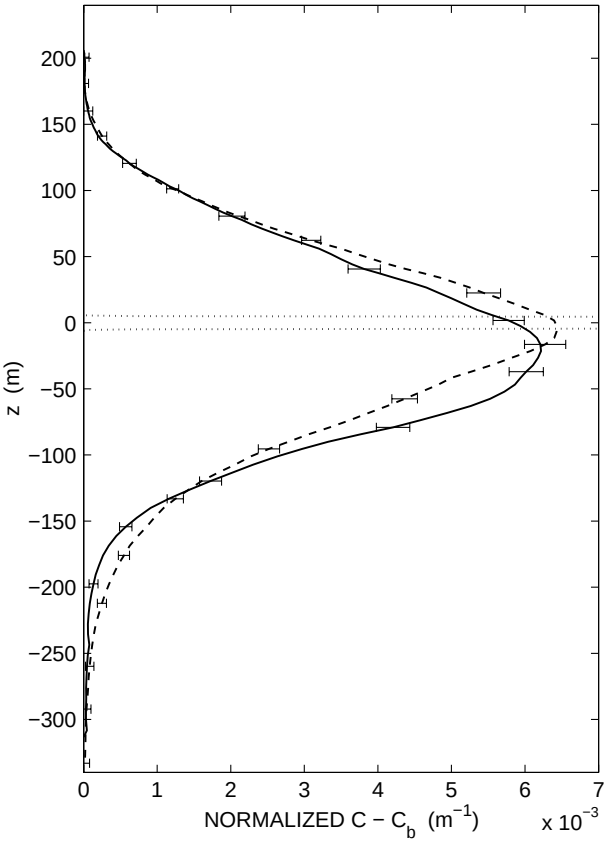

Fig. 3. Average vertical distribution of tracer about the injection density surface east of the Caribbean (solid line) and within the Caribbean Sea (dashed line) after 10 months. Tracer concentrations have been normalized such that the vertical integral is unity. The dotted lines delimit the initial tracer distribution. Averaging was done in density space, and the profiles were converted to physical space through the mean density profile for the stations east of Barbados.

Table 1. Diffusivities for salt and heat estimated from HRP measurements of χ_θ, the dissipation rate of thermal variance and ε, the dissipation rate of kinetic energy (penultimate row) $\times$ 10⁴ m²/s. The separate formulae for salt fingering and turbulent interpretations of the data are given. The estimates are based on the mean quantities over all stations occupied during the fall cruise between the potential density surfaces of 1026.968 and 1027.128 kg/m³, as these surfaces represent the 1-SD spread of the tracer. The 95% confidence interval for each estimate is given in the bottom row, based on statistics of the observed microstructure variables (*24*). Additional systematic errors may arise due to the uncertainties in the constants of the formulae.

Finger formulae (for $R_\rho = 1.71$, $\gamma = 0.75$)				Turbulence formulae (for $R_f = 0.17$)			
K_S		K_θ		K_S		K_θ	
$\frac{R_\rho}{\gamma}\frac{\chi_\theta}{2\overline{\theta_z}^2}$	$\frac{R_\rho - 1}{1-\gamma}\frac{\varepsilon}{N^2}$	$\frac{\chi_\theta}{2\overline{\theta_z}^2}$	$\frac{\gamma}{R_\rho}\frac{(R_\rho - 1)}{(1-\gamma)}\frac{\varepsilon}{N^2}$	$\frac{\chi_\theta}{2\overline{\theta_z}^2}$	$\frac{R_f}{1-R_f}\frac{\varepsilon}{N^2}$	$\frac{\chi_\theta}{2\overline{\theta_z}^2}$	$\frac{R_f}{1-R_f}\frac{\varepsilon}{N^2}$
1.03	2.40	0.45	1.07	0.45	0.17	0.45	0.17
0.56–1.8	0.8–6.6	0.26–0.75	0.36–2.7	0.26–0.75	0.06–0.42	0.26–0.75	0.06–0.42

eterization of diapycnal mixing continues to be a major uncertainty in assessing the ocean's ability to sequester heat, pollutants, and carbon dioxide.

References and Notes

1. M. E. Stern, *Tellus* **12**, 172 (1960).
2. R. B. Lambert, W. Sturges, *Deep-Sea Res.* **24**, 211 (1977).
3. R. W. Schmitt, *J. Phys. Oceanogr.* **11**, 1015 (1981).
4. B. Ruddick, *J. Phys. Oceanogr.* **22**, 1274 (1992).
5. R. W. Schmitt, H. Perkins, J. D. Boyd, M. C. Stalcup, *Deep-Sea Res.* **34**, 1697 (1987).
6. M. Tsuchiya, L. D. Talley, *J. Geophys. Res.* **103**, 12,899 (1998).
7. A. P. S. Wong, G. C. Johnson, *J. Phys. Oceanogr.* **33**, 1493 (2003).
8. J. R. Ledwell, A. J. Watson, C. S. Law, *Nature* **364**, 701 (1993).
9. J. R. Ledwell, A. J. Watson, C. S. Law, *J. Geophys. Res.* **103**, 21,499 (1998).
10. K. L. Polzin, J. M. Toole, J. R. Ledwell, R. W. Schmitt, *Science* **276**, 93 (1997).
11. J. R. Ledwell, E. T. Montgomery, K. L. Polzin, R. W. Schmitt, J. M. Toole, *Nature* **403**, 179 (2000).
12. J. D. Boyd, H. Perkins, *Deep-Sea Res.* **34**, 337 (1987).
13. R. W. Schmitt, *Annu. Rev. Fluid Mech.* **26**, 255 (1994).
14. R. W. Schmitt, J. M. Toole, R. L. Koehler, E. C. Mellinger, K. W. Doherty, *J. Atmos. Ocean. Tech.* **5**, 484 (1988).
15. R. W. Schmitt, *Deep-Sea Res.* **26A**, 23 (1979).
16. R. Lueck, *Deep-Sea Res.* **34**, 1677 (1987).
17. G. Marmorino, W. K. Brown, W. D. Morris, *Deep-Sea Res.* **34**, 1667 (1987).
18. A. E. Gargett, R. W. Schmitt, *J. Geophys. Res.* **87**, 8017 (1982).
19. T. J. McDougall, *Deep-Sea Res.* **38**, 367 (1991).
20. T. R. Osborn, *J. Phys. Oceanogr.* **10**, 83 (1980).
21. T. Osborn, C. Cox, *Geophys. Fluid Dyn.* **3**, 321 (1972).
22. T. J. McDougall, in *Small-Scale Turbulence and Mixing in the Ocean*, J. N. a. B. Jamart, Ed. (Elsevier Oceanography Ser., vol. 46, Elsevier, New York, 1988), pp. 21–36.
23. L. St. Laurent, R. W. Schmitt, *J. Phys. Oceanogr.* **29**, 1404 (1999).
24. The 95% confidence limits for the diffusivities were calculated using a "bootstrap" method with the statistics of 1000 random subsamples of half of the 165 stations for each of the measured variables. This treats each station as independent but does not account for possible systematic errors in the flux ratio or flux Richardson number.
25. M. C. Gregg, T. Sanford, *Deep-Sea Res.* **34**, 1689 (1987).
26. M. E. Stern, *Deep-Sea Res.* **14**, 747 (1967).
27. J. M. Toole, D. T. Georgi, *Prog. Oceanogr.* **10**, 123 (1981).
28. C. J. Garrett, *J. Phys. Oceanogr.* **12**, 952 (1982).
29. W. J. Merryfield, *J. Phys. Oceanogr.* **30**, 1046 (2000).
30. T. M. Joyce, *J. Phys. Oceanogr.* **7**, 626 (1977).
31. R. Ferrari, K. Polzin, *J. Phys. Oceanogr.* (in press).
32. M. C. Gregg, *J. Geophys. Res.* **94**, 9686 (1989).
33. K. Polzin, J. M. Toole, R. W. Schmitt, *J. Phys. Oceanogr.* **25**, 306 (1995).
34. E. Kunze, in *Double-Diffusive Convection*, A. Brandt and J. Fernando, Ed. *Geophys. Monogr.* 94, 313 (1995).
35. R. W. Schmitt, in *Small-Scale Turbulence and Mixing in the Ocean*, J. N. a. B. Jamart, Ed. (Elsevier Oceanography Ser., vol. **46**, Elsevier, New York, 1988), pp. 435–452.
36. W. J. Schmitz, J. R. Luyten, R. W. Schmitt, *Bull. Mar. Sci.* **53**, 1048 (1993).

37. We wish to thank the captains and crews of the R/Vs *Oceanus* and *Seward Johnson* for consistently fine work throughout our cruises. We also thank D. Wellwood, T. Bolmer, T. Farrar, T. Donoghue, B. Guest, C. Sellers, S. Birdwhistell, S. Sutherland, A. deBoer, L. Houghton, S. Ledwell, A. Benitez, G. Hernandez, and R. Brathwaite for scientific assistance during the cruises. This work was supported by the National Science Foundation under grants OCE-0081502 and OCE-0350743. This is Contribution Number 11284 of the Woods Hole Oceanographic Institution.

14 December 2004; accepted 16 March 2005
10.1126/science.1108678

Insect-Resistant GM Rice in Farmers' Fields: Assessing Productivity and Health Effects in China

Jikun Huang,[1]* Ruifa Hu,[1] Scott Rozelle,[2] Carl Pray[3]

Although no country to date has released a major genetically modified (GM) food grain crop, China is on the threshold of commercializing GM rice. This paper studies two of the four GM varieties that are now in farm-level preproduction trials, the last step before commercialization. Farm surveys of randomly selected farm households that are cultivating the insect-resistant GM rice varieties, without the aid of experimental station technicians, demonstrate that when compared with households cultivating non-GM rice, small and poor farm households benefit from adopting GM rice by both higher crop yields and reduced use of pesticides, which also contribute to improved health.

Despite promises that GM crops could make a contribution to the reduction of hunger throughout the world, GM varieties are primarily used for industrial crops, such as cotton, and feed crops for animals (*1*–*3*). The difficulties of commercializing GM rice (and other food crops) appear to be causing declines in the amount and direction of public and private biotechnology research (*4*). Consequently, GM rice has not been commercialized anywhere in the world, and little is in the pipeline in most countries. Even China, a country that aggressively commercialized Bt cotton and invested heavily into research on GM food crops, has not commercialized any major food crops.

One reason that commercialization may not have proceeded is that there has been little independent evidence on whether GM food crops would really improve farmer welfare. This study's objective is to report on the results of an economic analysis that uses data from eight rice preproduction trial sites in China. We attempt to answer three questions: Does GM rice help reduce pesticide use in the fields of farmers? Do the new varieties of GM rice increase the yields for farmers? Are there any identifiable health effects on the farmers that adopt GM rice strains?

China's biotechnology research program has generated a wide array of new technologies, including several GM rice varieties (*5*). A number of GM rice varieties have entered and passed field and environmental release trials, and four varieties are in preproduction trials in farmers' fields. Two of the varieties—the two in which the scientists that developed the varieties gave our study team permission to undertake economic analysis—are the focus of this study (*5*). One variety, GM Xianyou 63, was created to be resistant to rice stem borer and leaf roller by insertion of a Chinese-created *Bacillus thuringiensis* (Bt) gene (*5*, *6*). The other variety, GM II–Youming 86, also was created to be resistant to rice stem borers, but in this case, the resistance was created by introducing a modifed cowpea trypsin inhibitor (CpTI) gene into rice (*5*–*8*). The insect-resistant GM varieties entered preproduction trials in 2001.

The nature of China's preproduction trial system has facilitated the analysis of the effect of insect-resistant GM rice on farm households before commercialization. The preproduction trials of GM Xianyou 63 are being conducted by farmers in seven villages in five counties in Hubei province. The trials for GM II–Youming 86 are being conducted in one village in Fujian province. In the preproduction villages, households were randomly selected to participate in the study. All of the farmers that were randomly selected did participate (i.e., there were no drop-outs), and so all farmers in the sample villages can be divided into two groups—adopters and nonadopters. Each adopter was provided with a fixed amount of insect-resistant GM rice seed. For households with limited land size, the seed was enough to cover all of their plots (henceforth, full adopters). Others received only enough to cover part of their plots (partial adopters). Except for being provided insect-resistant GM rice seed (at the same price as they would have paid for non-GM varieties), there were no subsidies, and adopters cultivated the insect-resistant GM rice without the assistance of technicians. Because farmers use their own periodic, in-field

[1]Center for Chinese Agricultural Policy, Institute of Geographical Sciences and Natural Resource Research, Chinese Academy of Sciences, Jia 11, Datun Road, Beijing 100101, China. [2]Department of Agricultural and Resource Economics, University of California, 1 Shields Avenue, Davis, CA 95616, USA. [3]Department of Agricultural, Food, and Resource Economics, Rutgers University, 55 Dudley Road, New Brunswick, NJ 08901–8520, USA.

*To whom correspondence should be addressed. E-mail: jkhuang.ccap@igsnrr.ac.cn

Enhanced Diapycnal Mixing by Salt Fingers in the Thermocline of the Tropical Atlantic

R. W. Schmitt, J. R. Ledwell, E. T. Montgomery, K. L. Polzin, and J. M. Toole

Science, 308 (5722), • DOI: 10.1126/science.1108678